Journal of Non-Crystalline Solids 381 (2013) 12–16

Contents lists available at ScienceDirect

Journal of Non-Crystalline Solids

journal homepage: www.elsevier.com/ locate/ jnoncrysol

Dehydroxilation and crystallization of glasses: A DTA study

D.C. Lago [a,*], M.O. Prado [a,b,c]

[a] Consejo Nacional de Investigaciones Científicas y Técnicas, Avda. Ezequiel Bustillo Km. 9,5. Código Postal 8400, San Carlos de Bariloche, Pcia. Río Negro, Argentina
[b] Departamento Materiales Nucleares, Centro Atómico Bariloche, Comisión Nacional de Energía Atómica, Avda. Ezequiel Bustillo Km. 9,5. Código Postal 8400, San Carlos de Bariloche, Pcia. Río Negro, Argentina
[c] Instituto Balseiro (Universidad Nacional de Cuyo, Comisión Nacional de Energía Atómica), Avda. Ezequiel Bustillo Km. 9,5. Código Postal 8400, San Carlos de Bariloche, Pcia. Río Negro, Argentina

ARTICLE INFO

Article history:
Received 5 July 2013
Received in revised form 31 August 2013
Available online 2 October 2013

Keywords:
Dehydroxilation;
Crystallization;
Yttrium aluminosilicate glass;
Differential Thermal Analysis

ABSTRACT

Differential thermal analysis (DTA) is a technique frequently used for the study of the crystallization kinetics of glass powders during sintering. The effect of specific surface area on crystallization kinetics has been reported earlier. It has been shown that there is a shift in the DTA crystallization peaks towards lower temperatures for smaller particle size. This paper analyzes how the dehydroxilation endothermic peaks that appear in DTA measurements depend on specific area and on the heating rate. Experiments were done on yttrium aluminosilicate, samarium aluminosilicate and soda-lime silica glasses, slabs and powders. We found that some of them exhibit a dehydroxilation endothermic peak that overlaps at different extent with the crystallization peak. The dehydroxilation peak is not detected when yttrium aluminosilicate glass powder is preheated at melting temperatures, or its surface is previously hydrated. For the yttrium aluminosilicate glass a dehydroxilation apparent activation energy of 255 ± 50 kcal mol^{-1} was obtained using the Kissinger plot.

1. Introduction

Differential scanning calorimetry (DSC) and differential thermal analysis (DTA) have been extensively used in the study of the crystallization kinetics of glasses. Barandiaran and Colmenero [1] used DTA runs to estimate the critical cooling rates of glasses. Cabral et al. [2] used DTA to study the stability on heating of glasses that nucleate homogeneously. Both last studies were run with glass slabs instead of powders in order to avoid surface crystallization.

There are other papers of DTA measurements, run on glass powders. One of them is that of R. Müller [3]. Müller presented a model for surface crystallization kinetics of glasses and compared the model results with experimental data on fresnoite glass. In Ref. [3], the model satisfactorily explains the shift towards lower temperatures of the crystallization DTA peaks for smaller powder particle size. Although not discussed in Ref. [3], DTA runs on some of the fresnoite glass powders exhibited an endothermic event before the crystallization peak, especially for particles with sizes of 112 and 65 micrometers. For particles of 1.25 micrometers no endothermic peak is seen.

In Ref. [4], C. Lara et al. studied the crystallization of RO–BaO–SiO_2 (R = Mg, Zn), and it is shown in their DTA runs that for R = Zn there is an endothermic peak before the crystallization one, but no when R = Mg.

In Ref. [5], Sung-Bum Sohn et al. studied the influence of CeO_2 addition on the crystallization behavior in the glass system MgO–Al_2O_3–SiO_2, and also showed an endothermic peak before the crystallization peak.

In Ref. [6], Reben M., in a thermal study of oxyfluoride glass with strontium fluoride, also found an endothermic peak before the crystallization exothermic event.

This endothermic peak before crystallization is generally not discussed in the glass literature although it is thoroughly studied in mineral structure works during heating [7,8]. Moreover, very often the temperature for crystallization start, T_S, is chosen at the minimum of the endothermic peak which we will show that is not correct.

2. Experimental

2.1. Glass preparation

Yttrium aluminosilicate glass samples were prepared with composition: $1Y_2O_3 \cdot 1Al_2O_3 \cdot 3SiO_2$ which corresponds approximately to the core of the ternary glassy domain [9]. Samarium aluminosilicate glass samples were prepared with composition: $1Sm_2O_3 \cdot 1Al_2O_3 \cdot 3SiO_2$.

In each case, a mixture of high purity oxide precursors was homogenized in a rotating mill and melted in a platinum crucible for 2 h at 1600 °C. The melt was poured on a stainless steel plate and immediately splat-cooled using a second steel plate. A fraction of the glass was separated and identified as slab. The remainder glass was milled and sieved to obtain three different powder size samples.

Soda-lime silica glass samples were prepared with composition $1Na_2O \cdot 1CaO \cdot 2SiO_2$ (NCS). The melting procedure was the same as detailed above, at a lower temperature (1500 °C).

* Corresponding author at: Centro Atómico Bariloche, Avenida Bustillo 9500, R8402AGP, S.C. de Bariloche, Río Negro, Argentina. Tel./fax: +54 294 4445241.
E-mail address: dlago@cab.cnea.gov.ar (D.C. Lago).

0022-3093/$ – see front matter © 2013 Elsevier B.V. All rights reserved.
http://dx.doi.org/10.1016/j.jnoncrysol.2013.09.008

2.2. Particle size distribution measurement

Glass pieces were milled in an RS 200 vibratory disk mill and sieved. In the case of the yttrium aluminosilicate (YAS), the glass fractions obtained were those remaining between the following pairs of sieves: 50 and 100 μm (fraction 1), between 25 and 37 μm (fraction 2), and less than 25 μm (fraction 3). The last particle size was obtained by wet sieving.

Samarium aluminosilicate glass and soda-lime silica glass particles between 25 and 37 μm sieves were collected.

The particle size distribution of the different glass fractions was measured by laser diffraction with a Mastersizer Micro Malvern Instrument, with simultaneously applied ultrasound to disaggregate particle clusters. The dispersive medium was distilled water.

2.3. Flame polished surface

Part of fraction 2 glass powder was spheroidized by passing by a propane–oxygen flame. Particle surface got flame polished.

2.4. Thermal and gravimetric simultaneous analysis

The sample weight and the DTA signal were simultaneously measured with a SDT-Q600 TA instrument.

Glass transition (T_g) and crystallization temperatures (T_X) were also determined. Measurements were done in alumina or platinum crucibles. The reference crucible was an empty crucible. Experiments were carried out up to 1300 °C with a heating rate of 10 °C min^{-1}, in a 100 ml min^{-1} flux of 5.0 purity nitrogen gas.

2.5. XRD sample characterization

Crystallinity analysis was carried out on powder samples with a Bruker D8 Advance diffractometer, at a wavelength of 0.154054 nm. Scans were performed in the range 10°–90° with a step size of 0.01° min^{-1}.

3. Results

3.1. Particle size distribution

Fig. 1 shows the particle size distribution for each of the YAS glass powder fractions. As acicular particles pass through the sieves, the measured particle ranges are broader than the expected distributions.

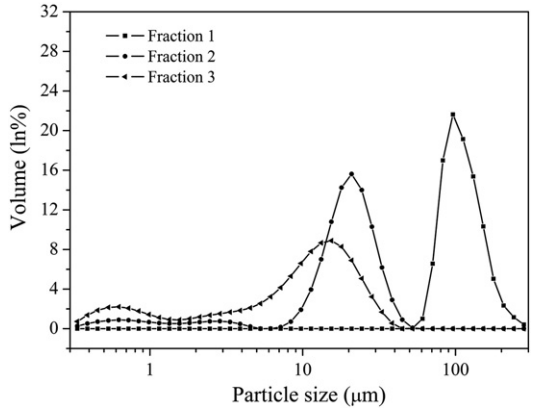

Fig. 1. Particle size distribution of different YAS glass powder fractions.

3.2. Differential thermal analysis

3.2.1. The effect of particle size distribution

Fig. 2 shows the DTA results for a monolith and the different fractions of YAS glass powder in alumina crucibles. The trace corresponding to the slab exhibits the T_g inflection and the crystallization peak as expected (being T_S the temperature corresponding to the start of the crystallization peak and T_X, the temperature of the peak maximum). The traces corresponding to glass powders present the same structure as for the slab, but moreover they have an endothermic peak at T_E.

The results of the DTA analysis are resumed in Table 1.

Fig. 3 shows the overlapping of the DTA trace for YAS fraction 3 and the cross section area of a powder cylinder during sintering in a hot stage microscope (HSM). Shrinking is previous to the endothermic peak.

3.2.2. The effect of annealing near T_g

In Fig. 4, we show the thermal behavior of YAS glass powder (fraction 2) as in Fig. 2, with legend 1a and 3a the effect of adding annealing 1 h and 3 h at 900 °C respectively. This was done in order to allow the system to stay some time in a viscoelastic region, during a characteristic time $t = \eta/G$. $\eta = 10^{13}$ Pa s and G is the shear modulus with an approximated value of 10^{10} Pa. This gives 1000 s as a characteristic relaxation time.

3.2.3. The effect of crucible chemical composition

In order to confirm that there was no chemical reaction between the glass powder sample and the alumina crucible, we repeated the measurement with particles between 25 and 37 μm (fraction 2) but this time in a platinum crucible (the results are shown in Fig. 4).

In order to discard the possible formation of crystalline phases during the endothermic peak, in one of the experiments the thermal heating was stopped at 1040 °C (just at the maximum of the endothermic peak), and the sample was quenched to room temperature at 50 °C min^{-1}. XRD was performed on the resulting sample.

3.2.4. The effect of particle surface quality

Since the DTA exothermic peak is observed with YAS glass powder, but not with the slab, the physical origin of this peak must be linked to glass surface properties. In order to explore this fact, in Fig. 5 we compare the DTA traces for YAS glass powder fraction 2, YAS glass powder fraction 2 + 30 h in distilled water at room temperature and YAS glass powder spheroidized in propane–oxygen flame.

The endothermic peak is well defined for the powder, but only suggested for powder that was in contact with water or that was passed through a propane–oxygen flame.

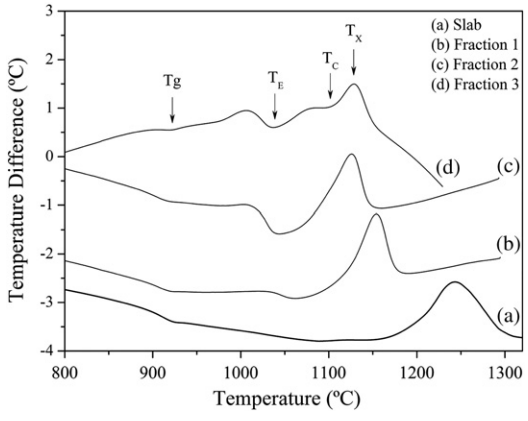

Fig. 2. DTA traces for slab and different YAS glass powder fractions. T_g, T_E, T_S and T_X are indicated.

Table 1
Glass transition and crystallization temperatures for different YAS fractions.

Sample	T_g (°C)	T_E (°C)	T_S (°C)	T_X (°C)
Slab	920	–	1148	1243
Fraction 1	919	1062	1057	1153
Fraction 2	917	1044	1037	1126
Fraction 3	922	1037	1033	1122

3.2.5. Other glasses

3.2.5.1. Samarium aluminosilicate glass. In this paper we also studied the DTA behavior of other glasses. Samarium aluminosilicate glass slab exhibits the same behavior as yttrium aluminosilicate glass slab; it does not present an endothermic peak previous to the crystallization peak. However, samarium aluminosilicate glass powder does (see Fig. 6), confirming the fact that the endothermic peak is a physical event linked to the specific surface area.

3.2.5.2. Soda-lime silica glass. A soda-lime metasilicate glass (NCS) was also tested. Fig. 7 shows the DTA trace for a slab and powder of a NCS glass. No endothermic peak is observed.

3.2.6. The effect of the heating rate on the endothermic reaction

For the YAS glass powder, fraction 2, DTA runs were done at 5, 10, 15, 20 and 40 °C min^{-1} (see Fig. 8). A Kissinger plot of the temperatures of maximum endothermic reaction rate is shown in Fig. 9. An apparent activation energy of 255 ± 50 kcal mol^{-1} is determined for the endothermic reaction.

3.2.7. Thermogravimetry

Fig. 10 shows thermogravimetric behavior of a YAS slab and of YAS powder with three different surfaces.

Let us remark that only YAS powder (b) exhibits endothermic peak in Fig. 5.

We assign the initial mass increase of the slab (a) to measurement error. Above T_g there is a mass decrease of about $1^{o}/_{oo}$ that we assign to a decrease in dissolved gases. For temperatures higher than T_S there is a slight mass decrease due to the decrease of gases solubility in the crystalline phases.

Glass microspheres (d) show at about 300 °C a slight mass decrease due to physical adsorbed water and again above T_g due to a decrease in dissolved gases. Both processes show very slight mass changes since during flame spheroidization most water and dissolved gases were expulsed.

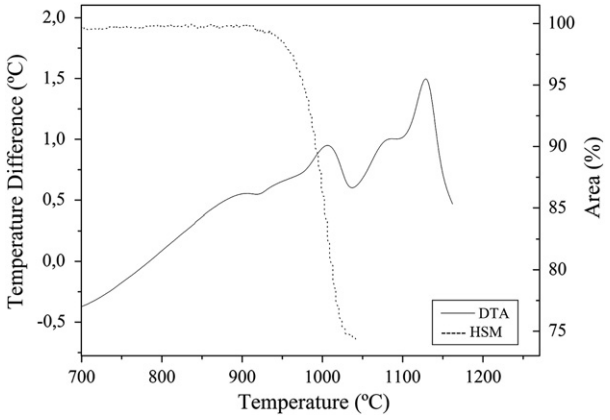

Fig. 3. Comparison of DTA and HSM curves on the same temperature scale for YAS glass powder (heating rate 10 °C min^{-1}). Solid line: DTA trace; dot line: HSM trace.

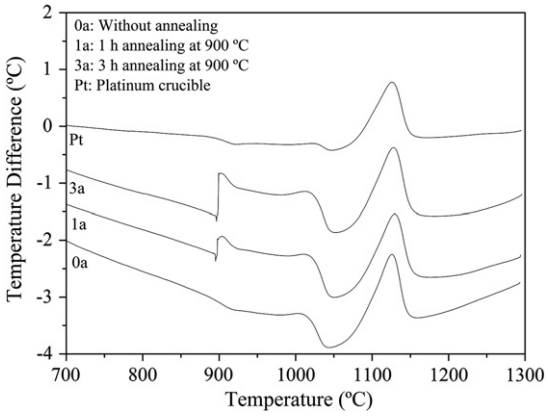

Fig. 4. 0a: thermal behavior of YAS glass powder (fraction 2). 1a: the same measurement, but adding an isothermal plateau at T_g = 900 °C during 1 h. 3a: isothermal plateau at 900 °C during 3 h. Pt: thermal behavior of YAS glass powder (fraction 2) in platinum crucible.

YAS powder (b) and YAS powder 30 h in water (c) show at about 300 °C a loss of adsorbed water, chemically adsorbed water at 600 °C and gas expulsion due to crystallization above 1122 °C.

From the results shown in this section, we do not detect a change of weight during the endothermic event. A simple calculation using Zhuravlev (Ref. [13]) data of maximum silanols (≡Si—OH) surface density equal to 5 ≡SiOH per nm^{-2} in silica, and considering that our composition is $1Y_2O_3 \cdot 1Al_2O_3 \cdot 3SiO_2$ and that 10% of surface Si has a silanol functional group, 3000 $cm^2 \cdot gr^{-1}$ sample specific surface area, and sample mass approximately 50 mg, shows that the mass loss during dehydration should be less than 0.3 micrograms, i.e. near the sensibility of our TG equipment.

4. Discussion

Fig. 2 shows a shift of the crystallization peaks of YAS powder samples towards lower temperatures as expected from Ref. [3]. However, the endothermic peaks exhibited by all the YAS powder samples except by the monolithic one are not explained in the literature.

The same occurs with SmAS glasses and other observed in this paper and the referenced literature.

The glass transition temperature is the same for all YAS samples, being in slab or powder form, suggesting that there has not been introduced glass structure changes during grinding. If grinding changed the glass structure by plastic deformation, this plastically deformed glass should have a different T_g value, and this is not observed. The glass transition temperature is maintained in all YAS samples, indicating that the supercooled liquid structure inherited is the same for all samples. We

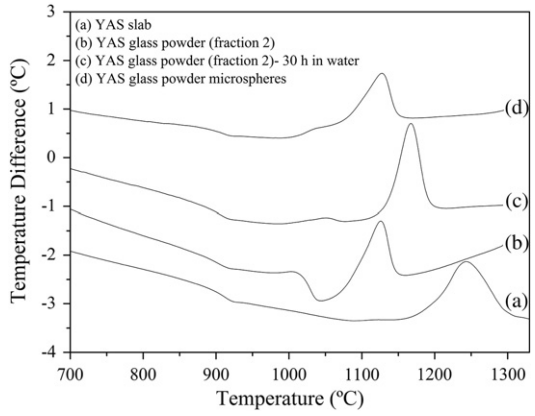

Fig. 5. DTA of YAS glass: (a) slab, (b) powder (fraction 2), (c) powder (fraction 2) + 30 h in contact with water at room temperature, (d) glass powder microspheres.

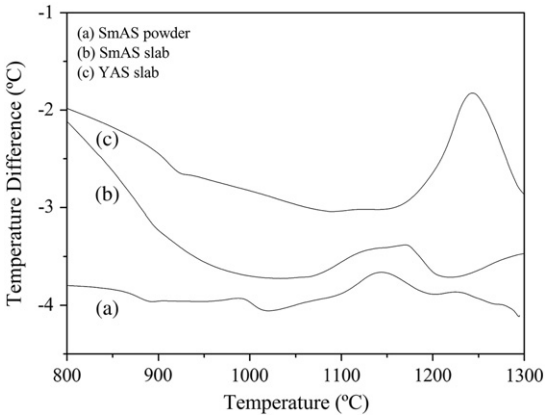

Fig. 6. DTA of (a) YAS glass slab, (b) SmAS glass slab and (c) SmAS glass powder showing the endothermic peak before crystallization.

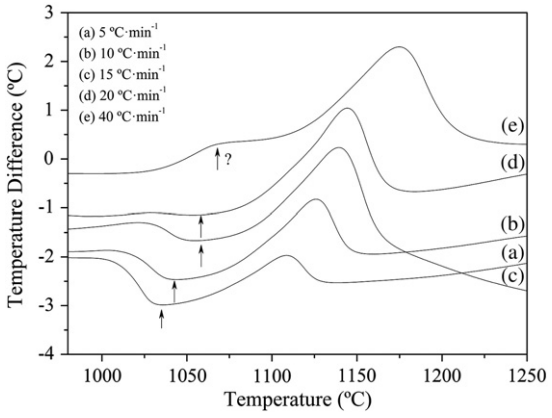

Fig. 8. Heating rate effect on the DTA results for YAS glass powder (fraction 2). The endothermic and the crystallization peak shifts towards higher temperatures with the increase of the heating rate.

note that the energy involved in this endothermic peak is comparable to the crystallization enthalpy.

The endothermic peak is due to a surface effect during heating of the crushed sample, since the monolithic sample does not present the endothermic behavior.

However, neither a soda-lime silicate glass powder nor a Pyrex glass powder tested in this work (DTA not shown in this work) exhibits endothermic peak (Fig. 7).

Moreover in the literature, some glass powder compositions exhibit a DTA endothermic peak [3-5] and some do not [10,11]. In Ref. [4], measurements on two sintering glass powders are shown; one of them exhibits endothermic peak and the other does not.

The partial overlapping of this peak with the crystallization peak complicates the interpretation of this evidence, which is more clear in the case of the YAS glass powder fraction 3 where the endothermic peak is well defined before the crystallization peak.

With YAS glass powders, the endo-peak is observable either using alumina crucibles or platinum crucibles, which eliminates the possibility that it is due to a sample-alumina crucible chemical reaction.

Moreover, the X-ray diffraction analysis confirms that within the limit of detection of XRD there is no crystallization at 1040 °C endothermic peak.

Fig. 5 shows that the endo-peak becomes sluggish when the YAS glass powder is passed through a propane–oxygen flame or when the powder is put for about 30 h in contact with distilled water.

It was shown for clays [7] that a possible reaction mechanism for dehydroxilation can be proposed. The proposed mechanism needs a proton delocalization at a specific hydroxyl site. For H_2O to form, the delocalized proton must migrate to a second hydroxyl site. If however, nonadjacent hydroxyls are involved, proton diffusion is needed, as was proved by the electrical conductivity increase in measurements done up to the dehydroxylation temperature.

We expect that the particles that were flame polished contain a lower surface density of silanols (≡Si—OH) which conducts to the almost absence of the endothermic peak (Fig. 5d). In the case of glass powder previously in contact with water (Fig. 5c), the increase of surface silanol density allows the condensation reaction [12,13]:

$$\equiv Si—OH + HO—Si\equiv \rightarrow \equiv Si—O—Si\equiv + H_2O\uparrow$$

to take place at lower temperatures, showing an important mass loss below 600 °C (Fig. 10c).

Thus, this surface endothermic reaction, with an apparent reaction enthalpy of 255 kcal mol^{-1} for YAS glass, as shown in Fig. 9, can be assigned to a dehydroxilation reaction. This value is in agreement with dehydroxilation measurements for clays [7].

5. Conclusions

The correct interpretation of the DTA/DSC experiments spectra is possible as long as we are aware of the different physical phenomena that occur during glass powder heating. Particularly, on studying glass powders crystallization, there is an effect on the crystallization peaks of moving toward lower temperatures, when compared with the results obtained with glass slabs.

Moreover when run on some glass powders, YAS glasses for example, DTA traces exhibit an endothermic peak before (or overlapped

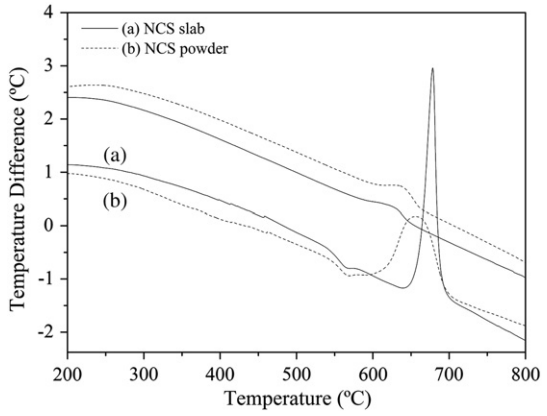

Fig. 7. DTA of (a) NCS glass slab, and (b) NCS glass powder showing the absence of an endothermic peak before crystallization.

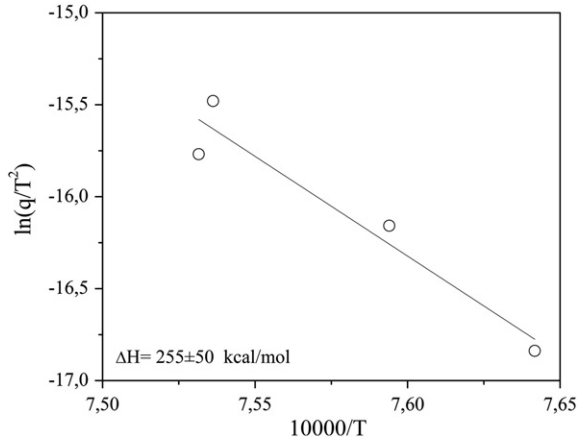

Fig. 9. Kissinger plot of YAS temperatures of maximum crystallization rates at different heating rates (data from Fig. 7).

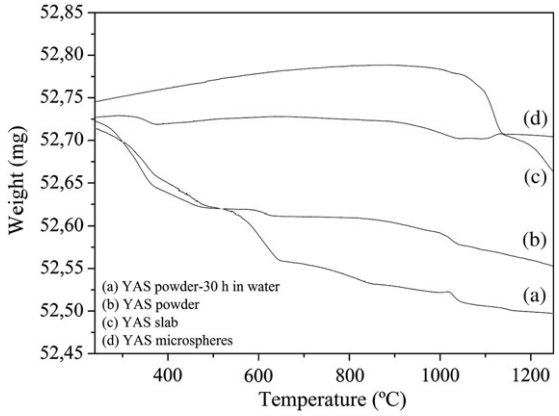

Fig. 10. Thermogravimetry of YAS samples with different surface quality.

with) the crystallization peak. This endothermic peak appears when we work with glass powders indicating that it is due to an endothermic surface process.

This endothermic peak has height, width and temperature span that depends upon the glass surface chemistry.

As the process is endothermic, it is not due to strain relaxation, crystallization (we checked experimentally this point with XRD just at the maximum of the endothermic peak) or available energy due to the sintering decreasing surface. Sintering can show a change in the DTA baseline but not an endothermic peak.

Since YAS glass components have a unique oxidation state, we do not expect an endochemical (or even exothermic) reaction to take place during the heating process.

The fact that flame spheroidized particles dramatically decrease the endothermic peak area suggests that the lower surface density of silanols results in a lower reaction heat consumption.

We determined that the apparent activation energy for this endothermic process is about 255 kcal mol^{-1}, which is in agreement with the dehydroxilation energy in clays.

In order to analyze a glass powder DTA, it is convenient to compare it with a slab DTA of the same glass, since in the latter surface effects are minimized.

Acknowledgements

This work has been financed by the project PICT 2008-39 ANPCyT Argentina.

References

[1] J.M. Barandiaran, J. Colmenero, J. Non-Cryst. Solids 46 (1981) 277–287.
[2] A. Cabral, A. Cardoso, E.D. Zanotto, J. Non-Cryst. Solids 320 (2003) 1–8.
[3] R. Müller, J. Therm. Anal. 35 (1989) 823–835.
[4] C. Lara, M.J. Pascual, A. Durán, J. Non-Cryst. Solids 348 (2004) 149–155.
[5] Sung-Bum Sohn, Se-Young Choi, J. Non-Cryst. Solids 282 (2001) 221–227.
[6] Manuela Reben, J. Non-Cryst. Solids 357 (2011) 2653–2657.
[7] R.L. Frost, A.M. Vasallo, Clay Clay Miner. 44 (5) (1996) 635–651.
[8] R.E. Grim, W.F. Bradley, Am. Mineral. 33 (1–2) (1948) 50–59.
[9] J.E. White, D.E. Day, Key Eng. Mater. 181 (1994) 94–95.
[10] Xiaojie J. Xu, Chandra S. Ray, Delbert E. Day, J. Am. Ceram. Soc. 74 (5) (1991) 909–914.
[11] Najim Sadiki, Jean Pierre Coutures, Catherine Fillet, Jean Luc Dussossoy, J. Nucl. Mater. 348 (2006) 70–78.
[12] Quan Wan, Christopher Ramsey, George Baran, J. Therm. Anal. Calorim. 99–1 (2010) 237–243.
[13] L.T. Zhuravlev, Colloids Surf. A Physicochem. Eng. Asp. 173 (2000) 1–38.